3D RECONSTRUCTION IN CRYO-EM BY RECOVERING ORTHOGONAL MATRICES

Author(s) Name(s)

Author Affiliation(s)

ABSTRACT

We present two new approaches for *ab-initio* modeling in single particle cryo-electron microscopy (Cryo-EM). The key idea, inspired from X-ray crystallography, is to use a previously solved structure which is similar to the unknown structure to be determined. The first approach, Orthogonal Extension, is powerful even in cases where the difference between the two structures is substantial, as confirmed by our numerical results. The second approach, Orthogonal Replacement, benefits from employing additional information from the experiment, resulting in a better reconstruction with a theoretical guarantee of exact recovery. We demonstrate the efficacy of our methods by numerical experiments on the simulated data of the Kv1.2 potassium channel.

Index Terms— Cryo-electron microscopy, semidefinite programming, single particle reconstruction, least quares, 3D.

1. INTRODUCTION

Cryo-electron microscopy is a popular technique in structural biology, used to determine the 3D structure of macromolecular complexes that are resistant to crystallization. The dataset consists of a large (typically 10^5 to 10^6) number of very noisy images taken at unknown angles. Reconstruction of small complexes is especially challenging and remains a long-standing problem in cryo-EM that poses a limit on its applicability. There exist many algorithms that, given a starting 3D structure, are able to refine it on the basis of cryo-EM images. All these require an *ab-initio* estimate of the structure as the starting point of the refinement process. When the particles are too small and images too noisy, the final result of the refinement process depends heavily on the choice of the initial model, which makes it crucial to have a good initial model. If the molecule is known to have a preferred orientation, then it is possible to find an *ab-initio* 3D structure using the random conical tilt method [1, 2]. There are two known approaches to the *ab-initio* estimation problem of the 3D structure that do not involve tilting: 1) the method of moments [3, 4] and 2) common-lines based algorithms. The method of moments is very sensitive to errors in the data and is of rather academic interest [5, section 2.1, p. 251]. Using common-lines based approaches, [6] were able to obtain three-dimensional *ab-initio* reconstructions from real microscope images of large complexes that had undergone only rudimentary averaging. Yet, even with such advanced averaging and common-lines based approaches, researchers have so far been unsuccessful in obtaining meaningful 3D *ab-initio* models directly from raw images that have not been averaged, especially for small complexes.

The key idea in both methods presented in this paper is inspired from the technique of 'molecular replacement', widely used in X-ray crystallography. The requirement for our methods to succeed is that the number of collected images is large enough for PCA of the 2D images to give non-trivial eigenimages (i.e., visible gap in the spectrum of the eigenvalues of the covariance matrix).

Thanks to XYZ agency for funding.

2. EXTENDING KAM'S THEORY

Kam showed [7] using the Fourier projection slice theorem that if the viewing directions of the projection images are uniformly distributed, then the autocorrelation function of the 3D volume with itself over the rotation group SO(3) can be directly computed from the covariance matrix of the 2D images, i.e. through PCA. Suppose $\phi(x, y, z)$ is a structure whose 3D Fourier transform is $\hat{\phi}(k_x, k_y, k_z)$. The expansion in spherical coordinates is given by $\hat{\phi}(k, \theta, \psi) = \sum_{l=0}^{\infty} \sum_{m=-l}^{l} A_{lm}(k) Y_l^m(\theta, \psi)$ where $k = \sqrt{k_x^2 + k_y^2 + k_z^2}$ is the radial frequency and Y_l^m are the spherical harmonics. Kam showed that we can extract the autocorrelation matrices C_l from the covariance matrix of the 2D Fourier transform of the projection images. For images sampled on a Cartesian grid we have

$$C_l = A_l A_l^* \tag{1}$$

where C_l is of size $K \times K$, K being the maximum frequency that depends on experimental settings, and A_l is of size $K \times (2l + 1)$, where the m'th column of A_l is the vector A_{lm}, and the rows of A_l are indexed by the radial frequency k. In practice, we calculate the l-subspace contribution C_l using the procedure outlined in [7]. However, the factorization of C_l is not unique. If A_l satisfies (1), then for any $(2l + 1) \times (2l + 1)$ unitary matrix U, $A_l U$ also satisfies (1). So from the sample covariance matrix of the 2D projection images, which is calculated following the steerable PCA procedure in [8],

we can retrieve the radial functions $A_{lm}, m = -l, \ldots, l$ for each l, up to a unitary matrix in $U(2l+1)$, where $U(2l+1)$ denotes the group of unitary matrices of size $(2l+1) \times (2l+1)$. This serves as a considerable reduction of the parameter space. Originally, we required $2l+1$ functions of the radial frequency for each l in order to completely characterize the structure ϕ. With the additional knowledge of C_l, however, our parameter space is reduced to $U(2l+1)$.

2.1. Relation to X-ray Crystallography

The missing unitary matrix above is reminiscent of the situation in X-ray crystallography, where the measured diffraction patterns contain information about the modulus of the 3D Fourier transform of the structure. However, the phases of the Fourier components are missing and need to be obtained by some other means. The missing unitary matrices in Kam's method and the missing phases in X-ray crystallography arise due to fundamentally different reasons. In crystallography, the particle's orientations are known but the phases are missing from the diffraction patterns, while in electron microscopy, the images do contain phase information but the orientations of the particles are missing.

2.2. Recovering Orthogonal Matrices

Since ϕ, the electric potential induced by the molecule, is real-valued, its Fourier transformation $\hat{\phi}$ satisfies $\hat{\phi}(x,y,z) = \hat{\phi}^*(-x,-y,-z)$, or equivalently, $\hat{\phi}(k,\theta,\psi) = \hat{\phi}^*(-k,\pi-\theta,\psi+\pi)$. Using this along with the properties of the real spherical harmonics, we obtain that $A_{lm}(k)$ (and therefore A_l) is real for even l and purely imaginary for odd l. Then A_l is unique up to a $(2l+1) \times (2l+1)$ orthogonal matrix $O_l \in O(2l+1)$, where $O(2l+1)$ denotes the group of $(2l+1) \times (2l+1)$ orthogonal matrices.

3. ORTHOGONAL EXTENSION (OE)

A classical solution to the missing phase problem in crystallography is 'molecular replacement'. In 'molecular replacement', one uses a previously solved homologous structure $\tilde{\phi}$ which is similar to the unknown structure ϕ whose diffraction patterns are measured. The structure is then estimated using the Fourier magnitudes from the diffraction data along with the phases from the known homologous structure. In analogy, we graft the orthogonal matrices of the already resolved similar structure onto the unknown structure. Suppose we have an unknown structure ϕ and a homologous complex with a known, similar structure $\tilde{\phi}$. The spherical harmonic expansion of the 3D Fourier transform of the known structure $\tilde{\phi}$ is given by

$$\hat{\tilde{\phi}}(k,\theta,\psi) = \sum_{l=0}^{\infty} \sum_{m=-l}^{l} \tilde{A}_{lm}(k) Y_l^m(\theta,\psi) \qquad (2)$$

We can obtain the auto-correlation matrices C_l from the cryo-EM images of the unknown structure using Kam's method. Let F_l be any matrix satisfying $C_l = F_l F_l^\star$, determined from the decomposition of C_l. Then $A_l = F_l O_l$, where $O_l \in O(2l+1)$. We estimate O_l by a least squares fit, i.e, by solving the minimization problem

$$O_l = \underset{O \in O(2l+1)}{\operatorname{argmin}} ||F_l O - \tilde{A}_l||_F^2 \qquad (3)$$

Although the orthogonal group is non-convex, this has a closed form solution given by $O_l = \tilde{V}_l \tilde{O}_l^T$, where $\tilde{O}_l \tilde{\Sigma} \tilde{V}_l^T$ is the SVD of $\tilde{A}_l^\star F_l$. Thus, we estimate A_l by $A_l = F_l \tilde{V}_l \tilde{O}_l^T$. In analogy with crystallography, the phase information $(\tilde{V}_l \tilde{O}_l^T)$ from the resolved homologous structure appends the experimentally measured intensity information F_l. Crystallography employs magnitude correction schemes such as setting the magnitude to be twice the magnitude from the desired structure minus the magnitude from the known structure, sometimes called 'twicing'. This has the desired effect of properly weighting the difference between the two structures, but also the undesired effect of doubling the noise level. For our numerical experiments, we employ the cryo-EM analog which is estimating A_l by $A_l = 2F_l \tilde{V}_l \tilde{O}_l^T - \tilde{A}_l$.

4. ORTHOGONAL REPLACEMENT (OR)

For many complexes it is typically not common to have a previously known homologous structure, which calls for a more general approach. OR can be employed even when there does not exist a homologous structure, making it more powerful than OE. Suppose $\phi^{(1)}(x,y,z)$ and $\phi^{(2)}(x,y,z)$ are two unknown structures for which cryo-EM images can be obtained. We assume that their difference $\Delta\phi = \phi^{(2)} - \phi^{(1)}$ is known. This occurs, for example, when an antibody fragment of a known structure binds to a protein. We acquire two sets of cryo-EM images, one from the protein alone, $\phi^{(1)}$ and another from the protein plus the antibody, $\phi^{(2)}$. Let $C_l^{(i)}$ be the matrices computed from the sample covariance matrices of the 2D projection images of $\phi^{(i)}, (i = 1, 2)$. Let $F_l^{(i)}$ be any matrix satisfying $C_l^{(i)} = F_l^{(i)} F_l^{\star(i)}$. Then, $A_l^{(i)} = F_l^{(i)} O_l^{(i)}$, where $O_l^{(i)} \in O(2l+1)$. The matrices $O_l^{(i)}$'s need to be determined for $i = 1, 2$ and $l = 0, 1, 2, \cdots$. Although both $A_l^{(1)}$ and $A_l^{(2)}$ are unknown, their difference $A_l^{(2)} - A_l^{(1)}$ is known from the 3D Fourier transform of the binding structure $\Delta\phi$. Thus for each l we obtain

$$A_l^{(2)} - A_l^{(1)} = F_l^{(2)} O_l^{(2)} - F_l^{(1)} O_l^{(1)} \qquad (4)$$

4.1. Relaxation to a Semidefinite Program

We can estimate $O_l^{(1)}$ and $O_l^{(2)}$ using ordinary least squares. The least squares problem

$$\underset{O_l^{(1)},O_l^{(2)}\in O(2l+1)}{\operatorname{argmin}} \quad ||A_l^{(2)}-A_l^{(1)}-F_l^{(2)}O_l^{(2)}-F_l^{(1)}O_l^{(1)}||_F^2 \quad (5)$$

is a non-convex optimization problem with no closed form solution and cannot be solved efficiently. We find $O_l^{(1)}$ and $O_l^{(2)}$ using a convex relaxation of (5) to a semidefinite program (SDP). We first homogenize (4) by introducing a slack unitary variable $O_l^{(3)}$ and considering the augmented linear system

$$(A_l^{(2)} - A_l^{(1)})O_l^{(3)} = F_l^{(2)}O_l^{(2)} - F_l^{(1)}O_l^{(1)} \quad (6)$$

If the triplet $O_l^{(1)}, O_l^{(2)}, O_l^{(3)}$ is a solution to (6), then the pair $O_l^{(1)}O_l^{T(3)}, O_l^{(2)}O_l^{T(3)}$ is a solution to the original linear system (4). The new associated least squares problem

$$\underset{\substack{O_l^{(1)},O_l^{(2)},O_l^{(3)}\\ \in O(2l+1)}}{\operatorname{argmin}} \quad ||(A_l^{(2)} - A_l^{(1)})O_l^{(3)} - F_l^{(2)}O_l^{(2)} - F_l^{(1)}O_l^{(1)}||_F^2 \quad (7)$$

is still non-convex. But it can be relaxed to a SDP. Let $Q \in \mathbb{R}^{3(2l+1)\times 3(2l+1)}$ be a symmetric matrix, which can be expressed as a 3×3 block diagonal matrix with block size $2l+1$, and the ij'th block given by $Q_{ij} = O_l^{(i)}O_l^{T(j)}$ for $i, j = 1, 2, 3$. It follows that $Q \succeq 0$. The eigenvalues of Q are all non-negative and $\operatorname{rank}(Q) = 2l+1$. All the $2l+1$ non-zero eigenvalues are equal to 3. The three diagonal blocks of Q are $Q_{ii} = I_{2l+1}(i = 1, 2, 3)$. The cost function in (7) is quadratic in $O_l^{(i)}(i = 1, 2, 3)$, so it is linear in Q. The problem can be equivalently written as: minimize $\operatorname{Tr}(CQ)$ over $Q \in (2l+1) \times (2l+1)$, subject to $Q_{ii} = I_{2l+1}$, $\operatorname{rank}(Q) = 2l+1$ and $Q \succeq 0$, where the matrix C can be written in terms of $A_l^{(2)} - A_l^{(1)}$, $F_l^{(1)}$ and $F_l^{(2)}$. Here, we have only one non convex constraint - the rank constraint. This constraint can be dropped to get a SDP that can be solved efficiently in polynomial time in l using existing software such as CVX [9]. We extract the orthogonal matrices $O_l^{(i)}$ from the decomposition of Q. If the solution matrix Q has rank greater than $2l+1$ (which is possible since we dropped the rank constraint), we use a singular value decomposition procedure [10] to find the closest orthogonal matrices.

4.1.1. Exact Recovery

For OR, we have theoretical guarantee on recovery of the $O_l^{(1)}$ and $O_l^{(2)}$ as follows.

Theorem 1. *Assume that $A_l^{(1)}$ and $A_l^{(2)} \in \mathbb{R}^{K\times(2l+1)}$ are elementwise sampled from i.i.d. Gaussian $N(0,1)$, and $K > 2l+1$, then the SDP method recovers $O_l^{(1)}$ and $O_l^{(2)}$ with probability* 1.

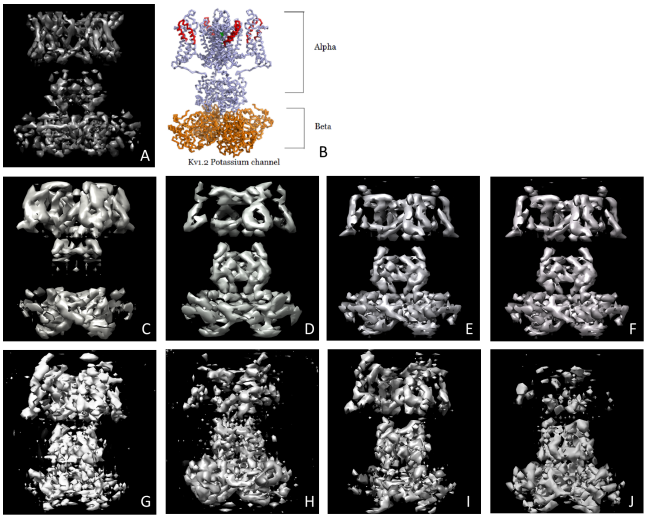

Fig. 1: Kv1.2 potassium channel: A) Volume visualization in UCSF Chimera [11]. B) Image from Protein Data Bank Japan (PDBj). C through F show reconstructions from clean images - C) OE with α_4 known, D) OE with β_4 known, E) OR with α_4 known, and F) OE with β_4 known. G through J show reconstructions from noisy images using OR - G) SNR=0.7 with α_4 known, H) SNR=0.7 with β_4 known, I) SNR=0.35 with α_4 known, and J) SNR=0.35 with β_4 known.

The proof of Theorem 1 is rather involved and we will put it in a separate work (Amit, what is the plan??- Teng) We remark that Theorem 1 also holds if $A_l^{(i)}$ are complex-valued and $O_l^{(i)}$ are unitary matrices. Theorem 1 shows that the power of the SDP method is close to the theoretical information limit since by counting the degrees of theorem, it is impossible to recover $O_l^{(1)}$ and $O_l^{(2)}$ if $K < 2l$.

4.2. Resolution Limit

(4) is a system of linear equations for $O_l^{(1)}$ and $O_l^{(2)}$ which can be estimated using least squares. The number of free parameters associated with an orthogonal matrix in $O(2l+1)$ is $l(2l+1)$. But the least squares method does not constrain $O_l^{(1)}$ and $O_l^{(2)}$ to $O(2l+1)$. Instead the solutions can be any square matrices of size $2l+1$. So the effective total number of variables for the least squares problem is $2(2l+1)^2$. The number of linear equations in (4) is $K(2l+1)$. Thus, using least squares we can resolve a truncated spherical harmonic expansion for $\phi^{(1)}$ and $\phi^{(2)}$ only for angular frequencies l that satisfy $K(2l+1) \geq 2(2l+1)^2$, that is, $l \leq \frac{K}{4} - \frac{1}{2}$. This introduces a natural resolution limit on structures that can be resolved. Ideally, we would like the least squares solution to take values in the orthogonal group since this would impose a less strict resolution limit on structures resolved, given by

$l \leq \frac{K}{2}$. Thus, we see that OR has the advantage of having an improved resolution limit.

5. NUMERICAL EXPERIMENTS

We present the results of numerical experiments on simulated images (109×109 pixels) of the Kv1.2 potassium channel complex (Fig. 1 A and B) and reconstruct its structure from clean and noisy projection images. The experiments were performed in MATLAB in UNIX environment on an Intel (R) Xeon(R) X7542 with 2 CPUs, having 6 cores each, running at 2.67 GHz, and with 256 GB RAM in total.

Kv1.2 is a dumbbell-shaped particle consisting of two subunits - a small β_4 subunit and a larger α_4 subunit, connected by a central connector. We performed experiments using OE and OR, assuming one of the subunits, for e.g. α_4, is known while the other, β_4, is unknown. In the case of OR, we additionally use projection images of the unknown subunit.

5.1. Clean and Noisy Projections

We reconstruct the structure from both clean and noisy projection images. The reconstruction of Kv1.2 obtained from clean images using OE and OR is shown in Fig. 1 C through F. We used the true C_l matrices for the known subunit, and a maximum l of 30. We tested OR to reconstruct Kv1.2 from noisy projections at various values of SNR. A sample projection image at different values of SNR is shown in Fig. 2. The C_l matrices were estimated from the noisy projection images. In Fig. 1 G through J we show the reconstructions obtained from 10000 projections using OR at SNR=0.7, and from 40000 projections using OR at SNR=0.35.

5.2. Comparison between OE and OR

We quantify the 'goodness' of the reconstruction using the Fourier Cross Resolution (FCR) [12]. FCR measures the normalized cross correlation between two 3D volumes over corresponding spherical shells in Fourier space - first, the reconstruction from noisy images, and second, the ground truth. In Fig. 3 we show the FCR curves for the reconstruction from the β_4 complex using OE and OR. The additional information in OR, from the projection images of α_4, results in a better reconstruction, as seen from the FCR curve. The Kv1.2 complex has $C4$ symmetry, which reduces the rank of the C_l matrices. Our experiment thus benefits from the reduced size of the orthogonal matrices to be recovered.

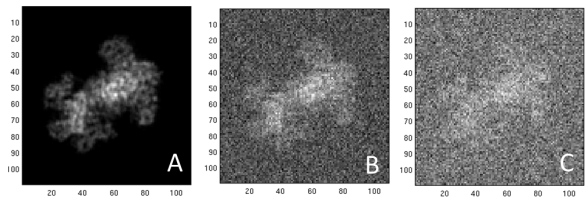

Fig. 2: Projection images at different values of SNR: A) Clean image, B) SNR=0.7, and C) SNR=0.35.

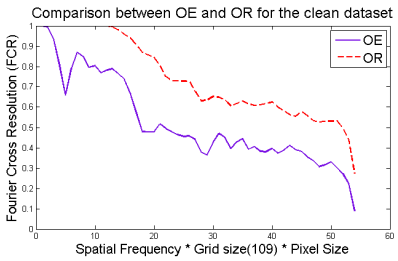

Fig. 3: FCR curve for reconstruction from β_4 (clean images)

5.3. Computational Complexity

The OE method requires the Cholesky decomposition of C_l and the SVD of $\tilde{A}_l^{\star} F_l$, which has a computational complexity of $O(K^3)$. The OR method requires solving a SDP problem of size $3(2l+1) \times 3(2l+1)$ with $3(l+1)(2l+1)$ linear constraints, and the theoretical running time of the interior point method is $O(l^{6.5})$ [13, Section 4.6.3]. In practice we use the MATLAB package CVX to solve the SDP. In our simulation with 10000 images, it took 416.36 seconds to perform steerable PCA and 194.04 seconds to calculate the C_l matrices (using the maximum l as 30). The running time to solve the SDP as a function of l is recorded in Table 1.

l	Time (seconds)
5	5.71
10	18.95
15	50.69
20	108.61
25	163.20
30	193.76

Table 1: Timing (in seconds) to solve the SDP with the MATLAB CVX package.

6. CONCLUSION

Reconstruction of small complexes is a long-standing problem in cryo-EM that poses a limit on its applicability. We expect the methods described in this paper to enhance the capabilities of three-dimensional electron microscopy techniques and be able to answer biological questions related to small protein structures that have so far remained unresolved. In the future, we plan to characterize the performance of these algorithms and their accuracy as a function of the number of images, the SNR, and the resolution, and test these methods on real datasets.

7. REFERENCES

[1] A. Verschoor M. Radermacher, T. Wagenknecht and J. Frank, "Three-dimensional reconstruction from a single-exposure, random conical tilt series applied to the 50s ribosomal subunit of escherichia coli," *Journal of Microscopy*, vol. 146, no. 2, pp. 113–136, 1987.

[2] A. Verschoor M. Radermacher, T. Wagenknecht and J. Frank, "Three-dimensional structure of the large ribosomal subunit from Escherichia coli," *EMBO J*, vol. 6, no. 4, pp. 1107–14, 1987.

[3] D.B. Salzman, "A method of general moments for orienting 2d projections of unknown 3d objects," *Comput. Vision Graph. Image Process.*, vol. 50, no. 2, pp. 129–156, May 1990.

[4] A.B. Goncharov, "Integral geometry and three-dimensional reconstruction of randomly oriented identical particles from their electron microphotos," *Acta Applicandae Mathematicae*, vol. 11, pp. 199–211, 1988.

[5] R.A. Grassucci P. Penczek and J. Frank, "The ribosome at improved resolution: New techniques for merging and orientation refinement in 3d cryo-electron microscopy of biological particles," *Ultramicroscopy*, vol. 53, no. 3, pp. 251 – 270, 1994.

[6] Z. Zhao and A. Singer, "Rotationally invariant image representation for viewing direction classification in cryo-em," *Journal of Structural Biology*, vol. 186, no. 1, pp. 153 – 166, 2014.

[7] Z. Kam, "The reconstruction of structure from electron micrographs of randomly oriented particles," *Journal of Theoretical Biology*, vol. 82, no. 1, pp. 15 – 39, 1980.

[8] Z. Zhao and A. Singer, "Fourier bessel rotational invariant eigenimages," *J. Opt. Soc. Am. A*, vol. 30, no. 5, pp. 871–877, May 2013.

[9] Michael Grant and Stephen Boyd, "CVX: Matlab software for disciplined convex programming, version 2.1," Mar. 2014.

[10] J. B. Keller, "Closest unitary, orthogonal and Hermitian operators to a given operator," *Mathematics Magazine*, vol. 48, pp. 192–197, 1975.

[11] Eric F. Pettersen, Thomas D. Goddard, Conrad C. Huang, Gregory S. Couch, Daniel M. Greenblatt, Elaine C. Meng, and Thomas E. Ferrin, "UCSF Chimera–a visualization system for exploratory research and analysis," *Journal of Computational Chemistry*, vol. 25, no. 13, pp. 1605–1612, 2004.

[12] Pawel A. Penczek, "Chapter three - resolution measures in molecular electron microscopy," in *Cryo-EM, Part B: 3-D Reconstruction*, Grant J. Jensen, Ed., vol. 482 of *Methods in Enzymology*, pp. 73 – 100. Academic Press, 2010.

[13] A. Ben-Tal and A. Nemirovski, *Lectures on Modern Convex Optimization: Analysis, Algorithms, and Engineering Applications*, MPS-SIAM Series on Optimization. Society for Industrial and Applied Mathematics (SIAM, 3600 Market Street, Floor 6, Philadelphia, PA 19104), 2001.